Signature: © Pol J Radiol, 2014; 79: 479-489
DOI: 10.12659/PJR.891107

Polish Journal of Radiology
www.PolRadiol.com
REVIEW ARTICLE

Received: 2014.05.29
Accepted: 2014.07.17
Published: 2014.12.21

Authors' Contribution:
A Study Design
B Data Collection
C Statistical Analysis
D Data Interpretation
E Manuscript Preparation
F Literature Search
G Funds Collection

Classical Signs and Appearances in Pediatric Neuroradiology: A Pictorial Review

Mehmet Haydar Atalar[ABCDEFG], **Ismail Salk**[DF], **Hulusi Egilmez**[BDE]

Department of Radiology, Cumhuriyet University, School of Medicine, Sivas, Turkey

Author's address: Mehmet Haydar Atalar, Department of Radiology, Cumhuriyet University, School of Medicine, Sivas, Turkey, e-mail: mhatalar@gmail.com

Summary

Radiological practice includes classification of illnesses with similar characteristics through recognizable signs. In this report, twenty-eight important and frequently seen neuroradiological signs in childhood are presented and described using X-rays, computed tomography (CT), magnetic resonance (MR) images, illustrations and photographs.

MeSH Keywords: Brain Diseases, Metabolic • Magnetic Resonance Imaging, Cine • Multidetector Computed Tomography • Nervous System Malformations

PDF file: http://www.polradiol.com/abstract/index/idArt/891107

Background

To correctly identify pediatric neuroradiological cases, radiologists should be familiar with the imaging characteristics and understand pathophysiological origins of these cases. Pediatric neuroradiology glossary has been gradually enriched with the explanations of the imaging findings commonly used in daily practice. Classical signs and appearances explaining these imaging findings assure radiologists about diagnosis. In this review, classical appearances and signs common to neuroradiology practice will be defined. Pathologies causing these appearances and signs and possible differential diagnoses will be discussed.

Classic Signs and Appearances

Ice-cream cone sign

It reflects normal appearance of incudomalleolar joint formed by malleolar head and body of the incus on axial computed tomography (CT) sections (Figure 1). Anatomical identification of this anatomic structure is important in terms of ossicular luxation especially in trauma cases. The space between the ice-cream cone and the scutum is called Prussak's space [1].

CT reversal sign

The reversal sign is associated with diffuse anoxic-ischemic brain damage and almost always observed in children (Figure 2). This sign is characterized by a relative reversal of the attenuation between supra- and infratentorial structures. The grey-white matter distinction is lost and decreased, and there is a diffuse decrease in density in the cerebral grey and white matter. Thalami, brainstem, and cerebellum have a relatively increased density. It is closely related to child abuse, especially when accompanying intracranial bleeding [1,2].

Mount Fuji sign

This sign is observed in bilateral subdural tension pneumocephalus. These air accumulations lead to compression in the frontal lobes and take a form of Mount Fuji on axial CT sections (Figure 3). It is most commonly seen after surgical decompression of chronic subdural hematoma. However, it may also be observed following a head trauma, otogenic infections, nitrous oxide anesthesia, and diving [3].

Lemon sign

The lemon sign is useful in identification of spina bifida and is commonly associated with hydrocephalus and Chiari II malformation. Loss of normal convex contour of the frontal bones in transverse fetal sonogram obtained at biparietal diameter (Figure 4). It has a high sensitivity and specifity in high-risk patients before the 24th gestational week. However, it is not specific for spina bifida and may be detected in encephalocele, Dandy-Walker malformation, thanatophoric dysplasia, cystic hygroma, corpus callosum agenesis, hydronephrosis, and umbilical vein varices [4].

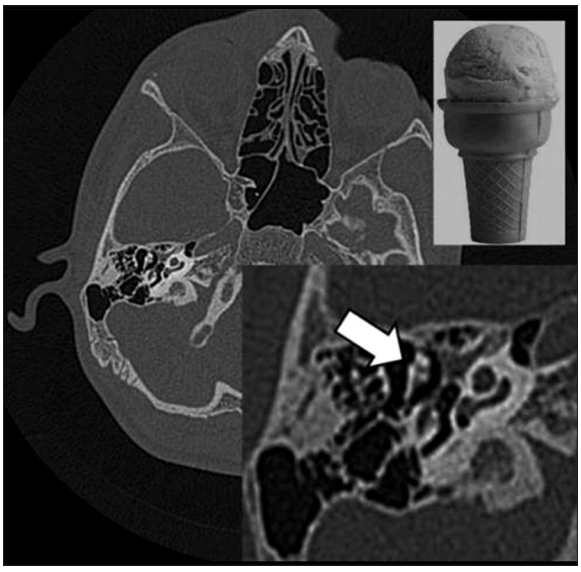

Figure 1. High resolution, axial CT image demonstrating the "ice-cream sign" of the temporal bone (white arrow). The sign represents the typical appearance of the malleoincudal joint.

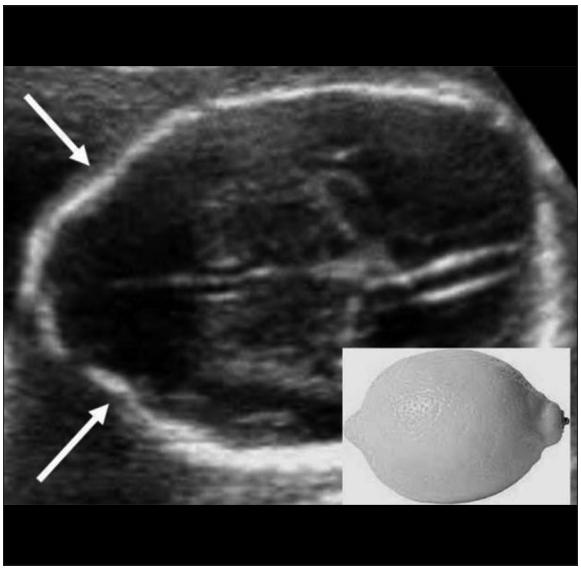

Figure 4. "Lemon sign" is seen in the frontal bones in a fetus with myeloschisis, as detected in an obstetrical US performed at the 20th week of gestation (white arrows).

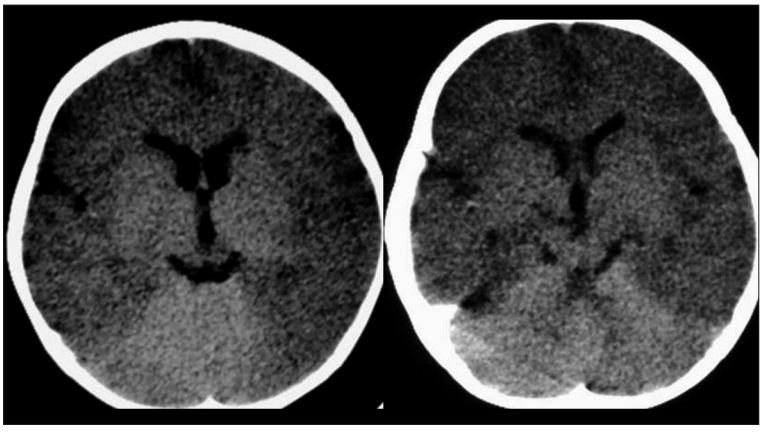

Figure 2. "CT reversal sign" is observed due to diffuse cerebral anoxia in non-contrasted CT examination.

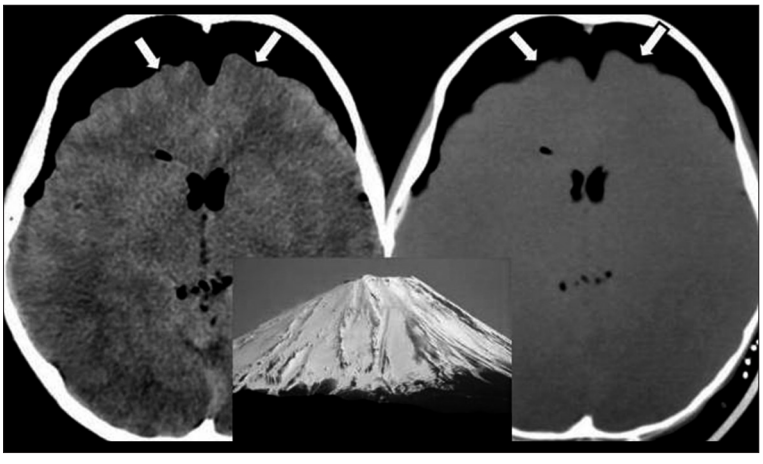

Figure 3. "Mount Fuji sign" due to tension pneumocephalus is observed in axial CT sections (parenchymal and bone window, white arrows)

Pancake brain sign

This sign defines the appearance of abnormal brain tissue in cases with alobar holoprosencephaly. Holoprosencephaly is an anomaly caused by a prosencephalic division defect and characterized by varying degrees of fusion of cerebellar hemispheres, diencephalon, basal ganglia, and thalami. The pancake brain sign is formed by fusion of cerebral hemispheres associated with the presence of typical monoventricle at the center (Figure 5) 1].

Figure 5. "Pancake brain appearance" formed by monoventricle cavity and cerebral hemispheric fusion is seen in T1-weighted MR image in a case with alobar holoprozencephaly.

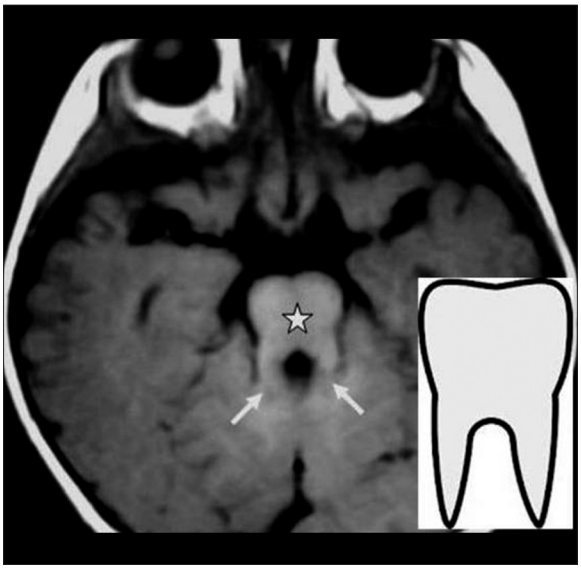

Figure 6. "Molar tooth sign" (star) at the level of pons and superior cerebellar peduncles coursing parallel to each other (white arrows) is seen in a T1-weighted MR section in a case with Joubert syndrome.

Molar tooth sign

Joubert syndrome is an autosomal recessive disorder characterized by abnormal eye movements, nystagmus, and difficulty in following mobile objects with eyes, apnea-tachypnea episodes, and motor retardation. Molar tooth sign represents abnormal antero-posterior orientation of superior cerebellar peduncles in a way similar to stems of a molar tooth on axial CT or magnetic resonance (MR) images (Figure 6). It is mainly observed in patients with Joubert syndrome [5,6].

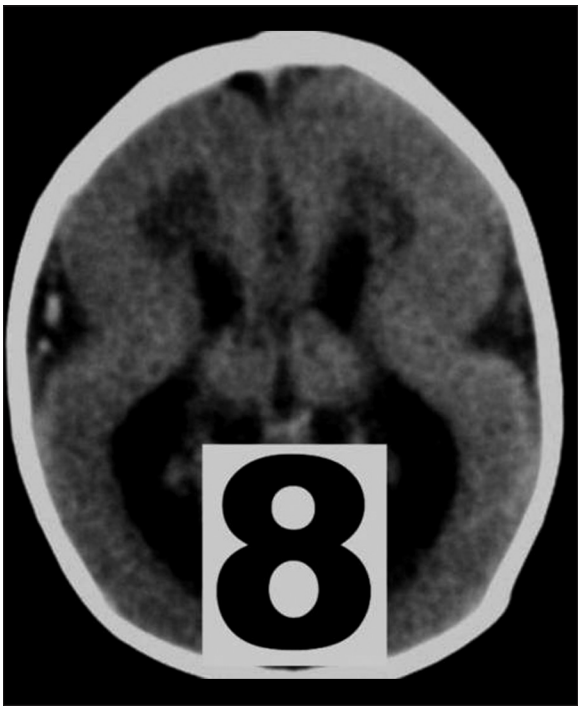

Figure 7. An appearance similar to "figure eight" due to lissencephaly in the axial plane on CT examination.

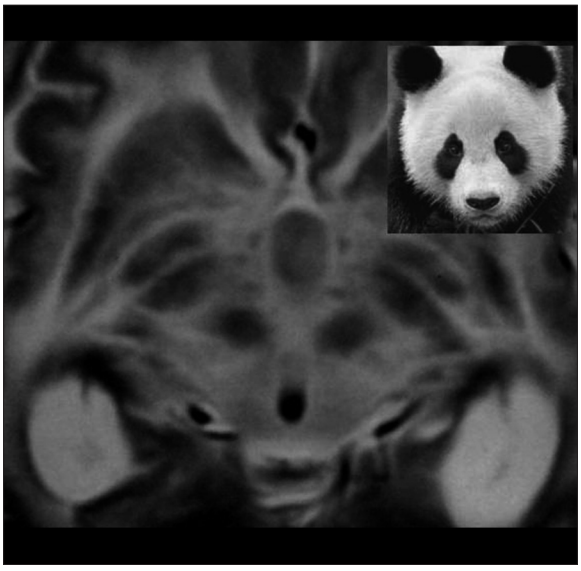

Figure 8. A "giant panda face" is observed in a T2-weighted axial MR image in a case with Wilson syndrome.

Figure eight sign

Lissencephaly is a disorder caused by defective neuronal migration between the 8-14th gestational week and characterized by a lack of development of gyri and sulci. Lissencephaly is classified into two subgroups: complete (type 1 – agyria) or partial (type 2 – pachygyria). Type 1 lissencephaly is characterized by shallow sylvian fissures that are vertically oriented. In this type of lissencephaly, brain takes on an hour-glass or figure-8 appearance due to compression at the middle part by sylvian fissures on axial imaging (Figure 7) [7].

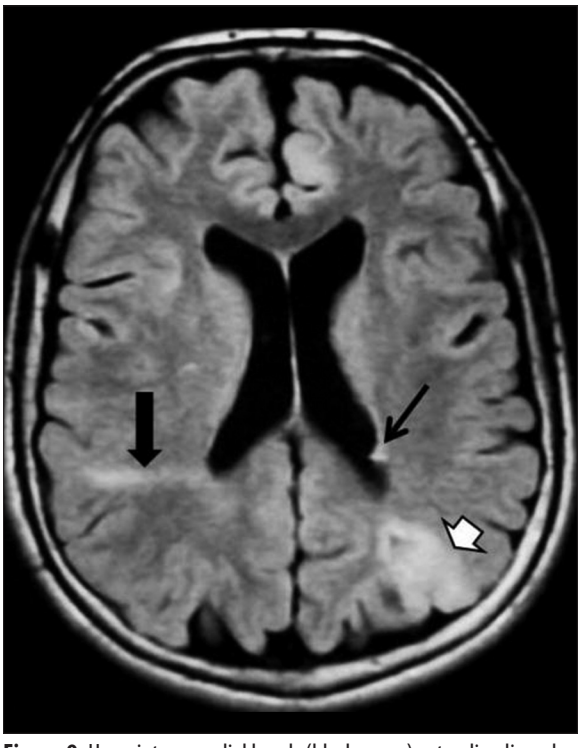

Figure 9. Hyperintense radial bands (black arrow) extending linearly at the level of the right cerebral hemisphere and a cortical tuber (short white arrow) located at the left parietal lobe in an axial FLAIR MR image in a case with tuberous sclerosis complex. In addition, MRI showing a subependymal nodule (thin black arrow).

Face of the giant panda sign

This sign was first described by Hitoshi et al. in Wilson's disease in 1991. It consists of high signal intensity in the tegmentum except for the red nucleus, preservation of signal intensity at the lateral portion of the pars reticulata of the substantia nigra, and hypointensity of the superior colliculus (Figure 8). The real pathology responsible for this appearance is the paramagnetic effect of the accumulation of heavy metals such as iron and copper in affected sites [8,9].

Radial band sign

Radial bands are linear or curvilinear areas with an abnormal signal intensity extending from the periventricular region to the subcortical region, that are best observed on T2-weighted (T2W) and especially FLAIR MR images (Figure 9). It is believed that radial band sign is indicative of abnormal migration of dysplastic stem cells during the course of radial glial-neuronal unit in patients with tuberous sclerosis complex. Radial bands are hypo-/isointense on T1-weighted images and hyperintense on T2W and FLAIR images [10].

String sign/Tigroid (Leopard skin) appearance

This sign is characterized by multiple dark spots or stripes (spared perivascular white matter) of normal white matter intensity scattered within the bright demyelinated periventricular white matter on T2W images (Figure 10). Tigroid appearance of the white mater has been found in some cases with Pelizaeus-Merzbacher disease and metachromatic leukodystrophy. However, it has been recently reported that it may be observed in cases with lissencephaly accompanied by cerebellar hypoplasia [11,12].

Open circle sign

The open ring sign is a relatively specific sign for demyelination, helpful in distinguishing between ring enhancing lesions. It is observed in patients with multiple sclerosis. It is observed as a lesion showing contrast effect as a circle that incompletely encircles a demyelinated plaque. The lesion is a high-intensity one on T2W images and it may be difficult to distinguish from an abscess or astrocytoma in this form (Figure 11) [13,14].

Light bulb sign

Diffusion-weighted (DW) MR imaging is the method that can delineate ischemic lesions in the brain at the earliest stage. With the help of this method, this lesion can be demonstrated after the onset of the event. The ischemic area shines like a light bulb at this stage (it appears darker on ADC images) (Figure 12). This area forms the core of the infarcted region. The brightness diminishes by the 2nd–3rd month. In this way, acute and chronic infracts can be

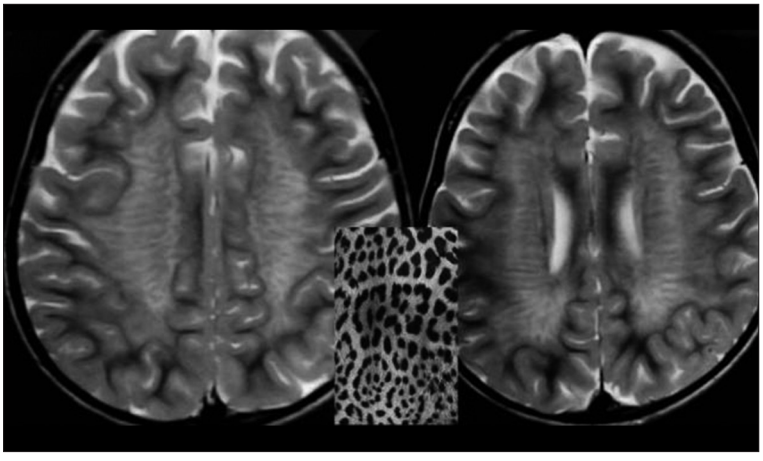

Figure 10. A "tigroid appearance" is observed at periventricular white matter in axial T2-weighted MR sections in a 2-year-old girl with metachromatic leukodystrophy.

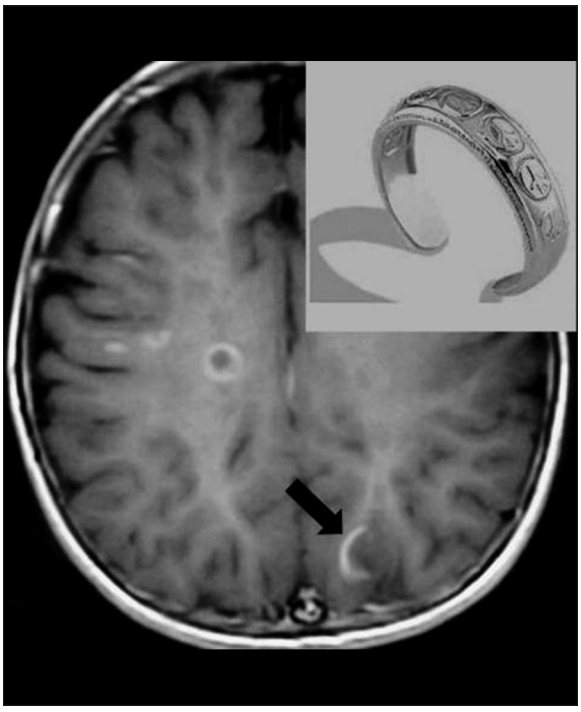

Figure 11. Post-contrast T1-weighted MR image showing an incomplete ring lesion enhancing in the right parietal region (black arrow).

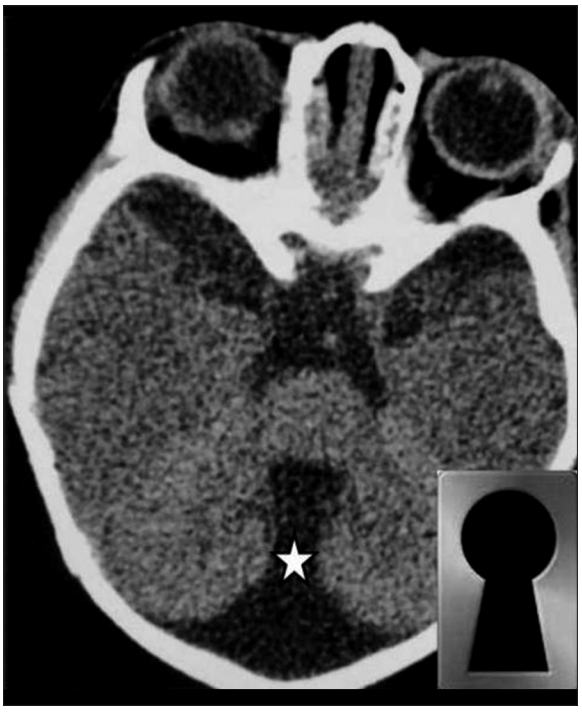

Figure 13. Axial non-contrast CT image showing typical "key-hole" appearance of cisterna magna communicating with a dilated 4th ventricle (star).

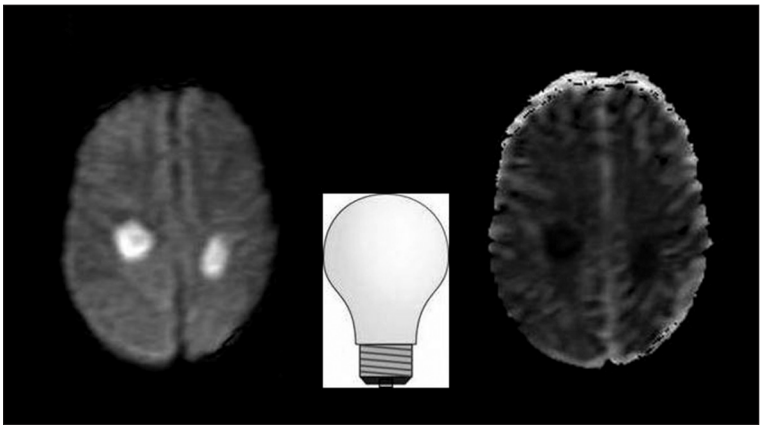

Figure 12. The b=1000 s/mm^2 DWI showing an acute infarct as "light bulb" bright.

distinguished or acute lesions can be defined in patients with multiple lesions of varying age. The marked increase in DWI signal in areas of acute ischemia, relative to unaffected brain, is typically so striking that this finding has been referred to as the "light bulb sign" of acute stroke [15].

Keyhole sign

The posterior fossa dimensions are normal in Dandy-Walker variants. There is a mild vermian hypoplasia and thus the vallecula becomes widened between the cerebellar hemispheres under the vermis. The fourth ventricle and cisterna magna communicate with each other through this wide vallecula. This appearance on axial CT and MR images is called "keyhole sign" (Figure 13) [16].

Dawson finger

It is detected on MR examination in multiple sclerosis. Demyelinating plaques are observed as focal signal areas on proton density and T2W MR images (Figure 14). These plaques are round or ovoid lesions limited particularly to the periventricular region. The appearance of periventricularly located ovoid lesions in the extended form along the ventricle is called Dawson finger [17].

Cortical vein sign

This was first described in MRI and also reported later on US and CT. It is used to differentiate extra-axial subarachnoid and subdural effusions from each other. On both CT and MRI, bridging veins extend from the cortical surface to the arachnoid (Figure 15). Appearance of bridging veins coursing in that manner in the extra-axial fluid is called

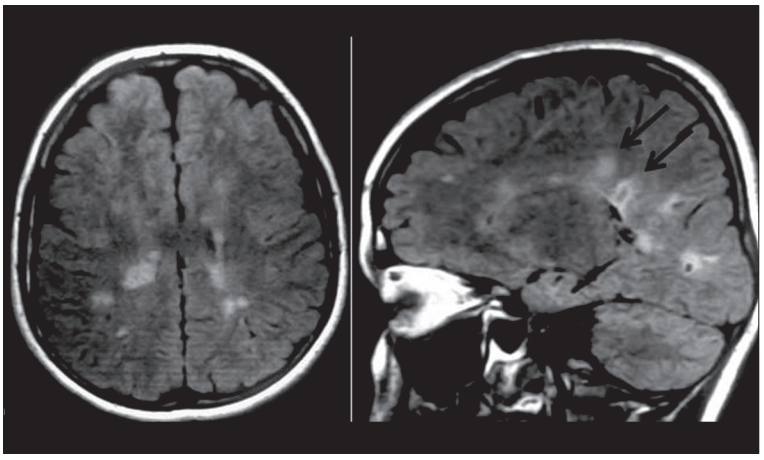

Figure 14. Axial and parasagittal FLAIR MR images demonstrating multiple sclerosis plaques extending up through the corpus callosum (thin black arrows).

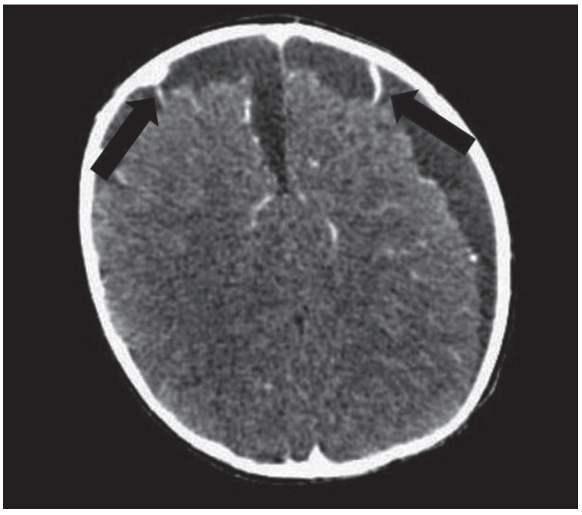

Figure 15. Post-contrast axial CT image showing the cortical veins (black arrows).

a positive cortical vein sign and indicates that the fluid is located subarachnoidally. The fluid is located subdurally when these veins are invisible [18].

Caput medusa sign

The most common vascular malformation in the bran is venous angiomas. They are most commonly observed in the frontal lobe and the posterior fossa. It has been suggested that they stem from a pause during brain development, i.e. when the arterial system completes its development but the venous system is not fully developed yet. The caput medusa sign, also known as a palm tree sign, refers to developmental venous anomalies of the brain, where a number of veins drain centrally towards a single drain vein. (Figure 16). The appearance is reminiscent of Medusa, a gorgon of Greek mythology, who was encountered and defeated by Perseus. The sign is seen on both CT and MRI when contrast is administered [19,20].

Angel wing sign

Chiari type II is the most common type of Chiari malformation. It is also known as Arnold-Chiari malformation. In 90% of cases there is also myelomeningocele,

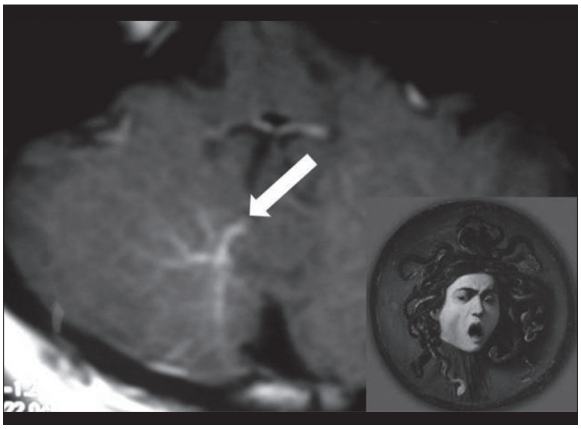

Figure 16. Contrast-enhanced T1-weighted axial MR image confirming converging tubular structures that represent a venous angioma (white arrow) in the medial aspect of the right cerebellar lobe.

Figure 17. Axial T2-weighted MR image showing an "angel wing appearance" in the brainstem (black arrows).

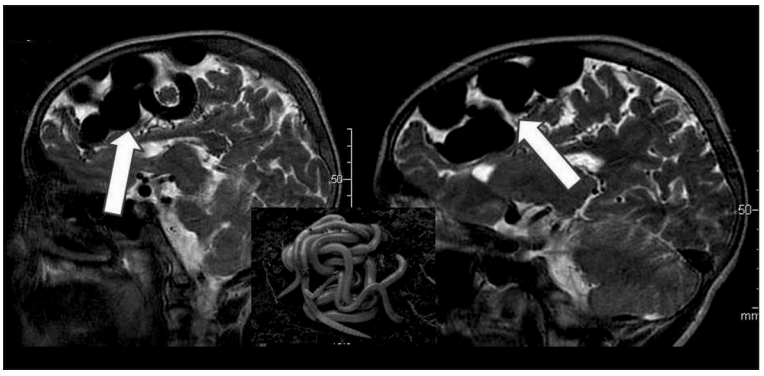

Figure 18. Sagittal T2-weigted MRI images showing a nidus of compact vessel with a typical appearance of "bag of black worms" in the left frontal region (white arrows).

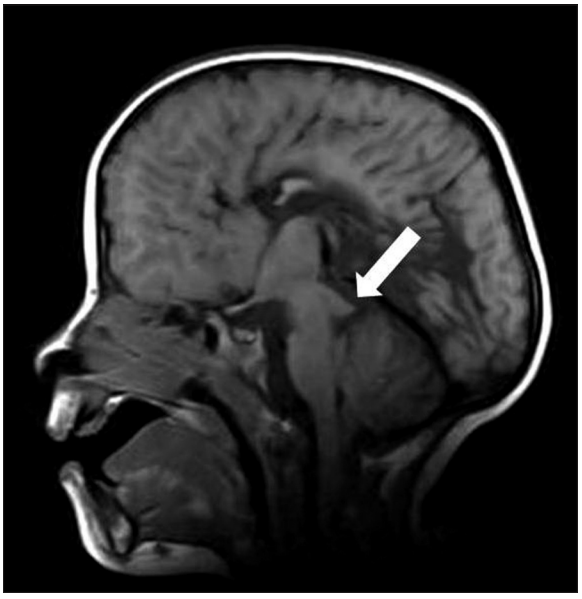

Figure 19. Sagittal T1-weighted MRI demonstrating a small posterior fossa with a low-lying tentorial attachment posteriorly. The tectum is beaked (white arrow) and partial corpus callosum agenesis is present.

hydrocephalus, and corpus callosum agenesis. In these cases, prepontine migration of the cerebellum at the level of the middle cerebellar peduncle gives the brainstem an angel wing appearance on axial MR images (Figure 17) [21].

Worm bag sign

Arteriovenous malformations are space-occupying lesions formed by conglomerated large vessels. There may sometimes be a very small amount of brain tissue between the vessels in intracranial arteriovenous malformations. There is no brain tissue at all in some cases. Thus, such an appearance of large vessels resembles clustered worms and is called a worm bag sign (Figure 18) [22].

Tectal beaking

Chiari type II is the most common type of Chiari malformation. It is also known as Arnold-Chiari malformation. In 90% of cases there is also myelomeningocele, hydrocephalus, and corpus callosum agenesis. Variable degrees of fusion of the colliculi and tectum result in prominent beaking and inferior displacement of the tectal plate. In these cases, the appearance of the pointed tectum is called tectal beaking (Figure 19) [21].

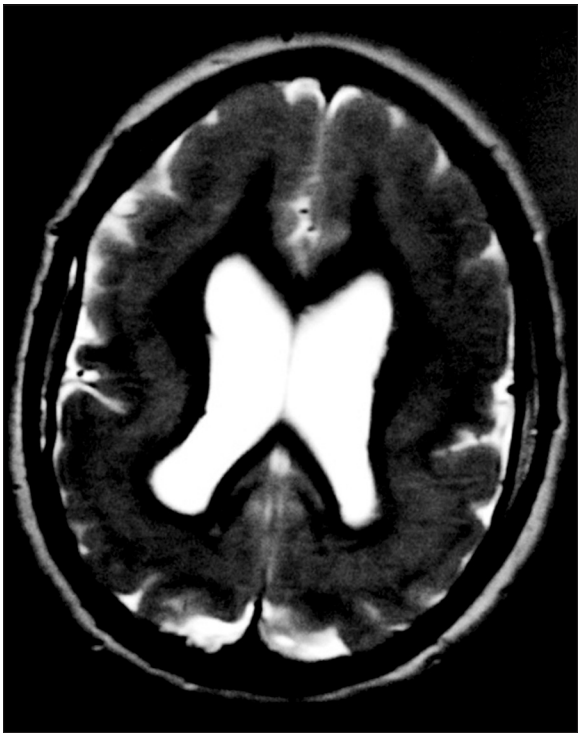

Figure 20. Axial T2-weighted MR image showing four layers consisting of cortex, thin outer white matter, diffuse subcortical heterotopia, and inner white matter around the lateral ventricles, giving the appearance of a "double cortex"

Double cortex appearance

Because of the early arrest of neuronal migration, a symmetric circumferential band of heterotopic grey matter is separated from the overlying cortex by a thin band of white matter. On MRI, the brain appears to have a "double cortex" appearance (Figure 20). The condition is quite rare, found predominantly in females, and is occasionally associated with an X-linked dominant inheritance pattern [23].

Banana cerebellum sign

The banana cerebellum sign is one of the many notable fruit-inspired signs, such as the "lemon sign". In neural

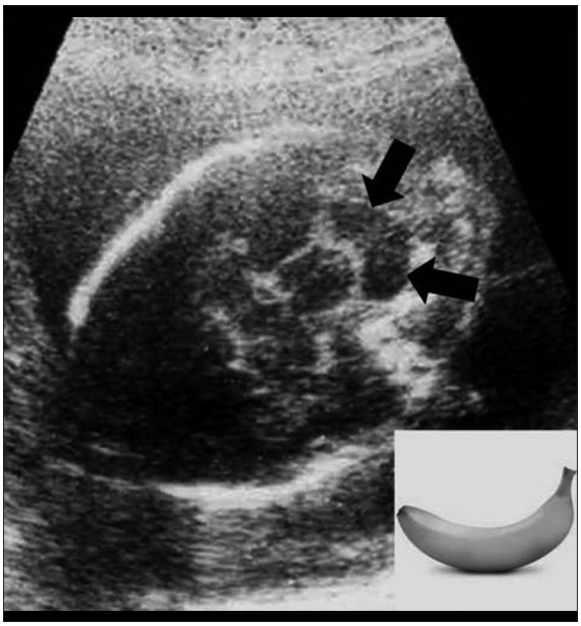

Figure 21. Transverse US image showing small posterior fossa and banana-shaped cerebellum ("banana sign") (black arrows.

tube defects, folding of the cerebellum around the posterior brain stem due to inferior traction of the spinal cord causes the cerebellum to take the form of a banana. It has been reported that it may be present in 57% of fetuses with neural tube defect. In fetal hydrocephalus, a cerebellar deformation is observed in conjunction with ventriculomegaly and deletion of cisterna magna. In these cases, the cerebellum loses its normal central convexity and becomes compressed parallelly to the occipital bone, resembling a banana (Figure 21) [24].

Viking helmet appearance

The "Viking helmet" appearance refers to the lateral ventricles in the coronal projection in patients with dysgenesis of the corpus callosum. The cingulate gyrus is everted into narrowed and elongated frontal horns (Figure 22). Dysgenesis of the corpus callosum may be complete (agenesis) or partial and represents an "in utero" developmental anomaly [25,26].

The Tram-Track sign

The tram-track sign is seen on skull radiographs as gyriform, curvilinear, parallel opacities that have the appearance of calcifications (Figure 23). A similar appearance can be seen on CTs. Sturge-Weber syndrome is a rare neurocutaneous syndrome that includes a facial port-wine stain and is associated with leptomeningeal angiomatosis. Weber demonstrated the characteristic gyriform intracranial calcifications. Calcifications are often gyriform and curvilinear and are most common in the parietal and occipital lobes. Calcifications can be more extensive but with frontal lobe and/or bilateral involvement. CT scans show calcifications in the areas of atrophy [27].

Diamond-shaped fourth ventricle

This appearance is seen in rhombencephalosynapsis. Rhombencephalosynapsis is a rare condition with most cases found in newborns and infants. Morphological

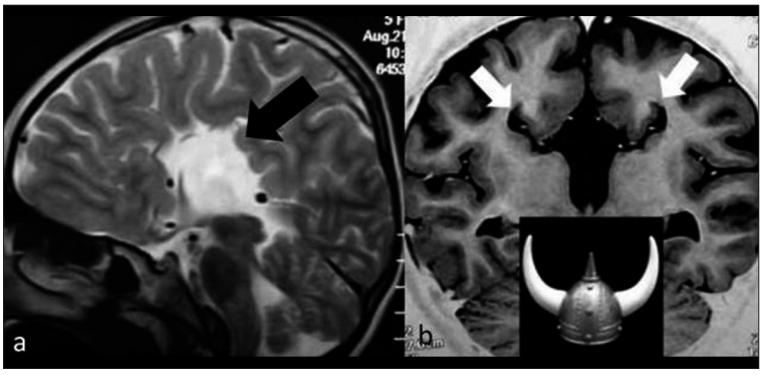

Figure 22. Coronal view of MRI head of the patient demonstrating the lateral ventricles forming a "Viking helmet" appearance (white arrows) due to the absence of corpus callosum (black arrow).

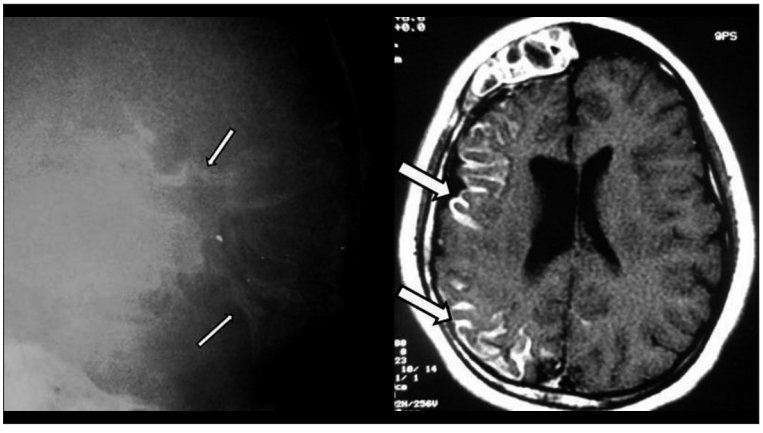

Figure 23. Lateral skull radiograph in a patient with Sturge-Weber syndrome showing parallel cortical calcifications (thin-white arrows). Contrast-enhanced axial T1-weighted MRI showing gyriform contrast enhancement in the right cerebral hemisphere (white arrows). There is brain atrophy on the right side. The cranial vault is asymmetric as secondary to brain atrophy.

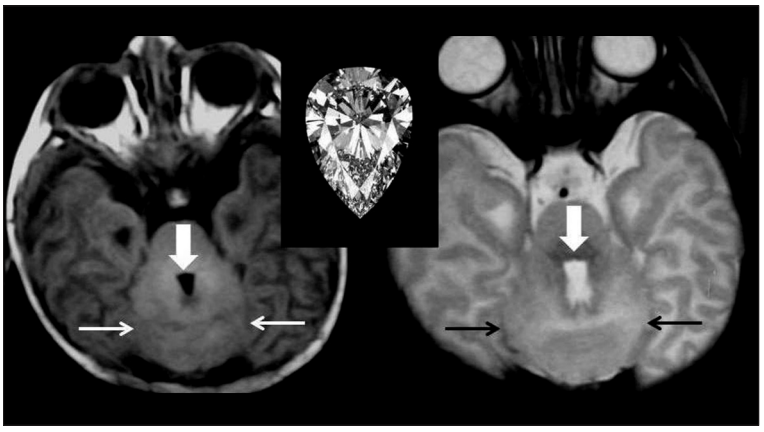

Figure 24. Axial T2-weighted MRI at the level of the posterior fossa showing antero-posterior elongation of the fourth ventricle giving it a "diamond shaped" appearance (arrows).

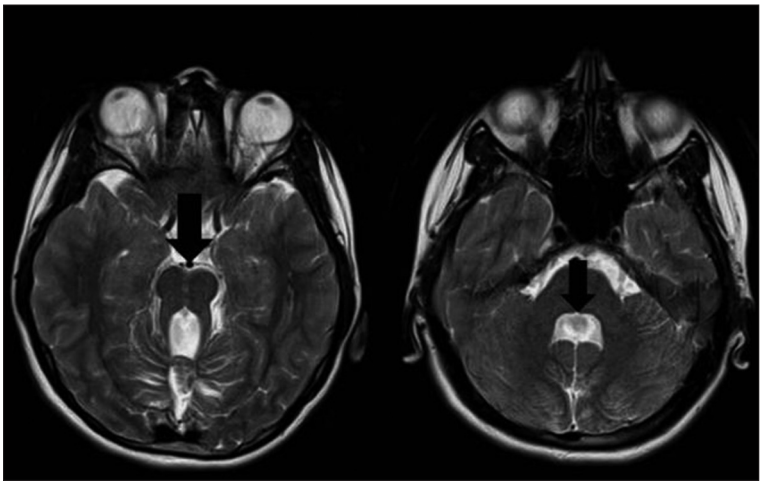

Figure 25. Axial T2-weighted MRI image at the level of the pontomedullary junction demonstrating the 4th ventricle that is shaped like a "bat wing" (arrow). In addition, axial T2-weighted MR image showing molar tooth sign (arrow).

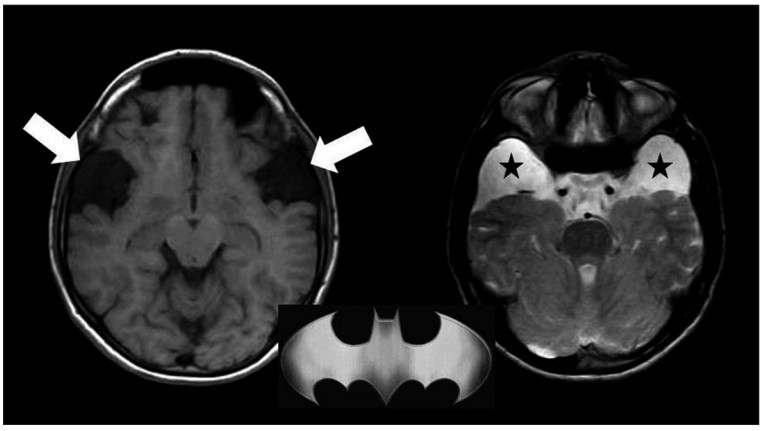

Figure 26. Axial T1-weighted and T2-weighted images demonstrating widened sylvian fissures producing "bat-wings" appearance (arrows and stars).

findings are predominantly characterized by fusion of the cerebellar hemispheres and absence of the vermis, often accompanied by supratentorial anomalies. The size of the fourth ventricle is variable and in its axial plane it usually has a "keyhole or diamond shape" (Figure 24). This appearance is a result of dorsal and rostral convergence of the dentate nuclei, cerebellar peduncles and inferior colliculi [28].

Bat wing 4th ventricle

Bat wing 4th ventricle sign refers to the morphology of the fourth ventricle in the Joubert anomaly and related syndromes. The absence of the vermis with apposed cerebellar hemispheres give the fourth ventricle an appearance reminiscent of a bat with its wings outstretched. It is best demonstrated in axial imaging (Figure 25) and could be easily missed in sagittal and coronal images [29].

Bat wing appearance of sylvian fissures

Glutaric aciduria type 1 (GA-1) is an autosomal recessive inborn error of lysine, hydroxylysine and tryptophan metabolism that results from a deficiency of glutaryl-CoA dehydrogenase. The most striking finding on brain imaging is the presence of very wide CSF spaces anterior to

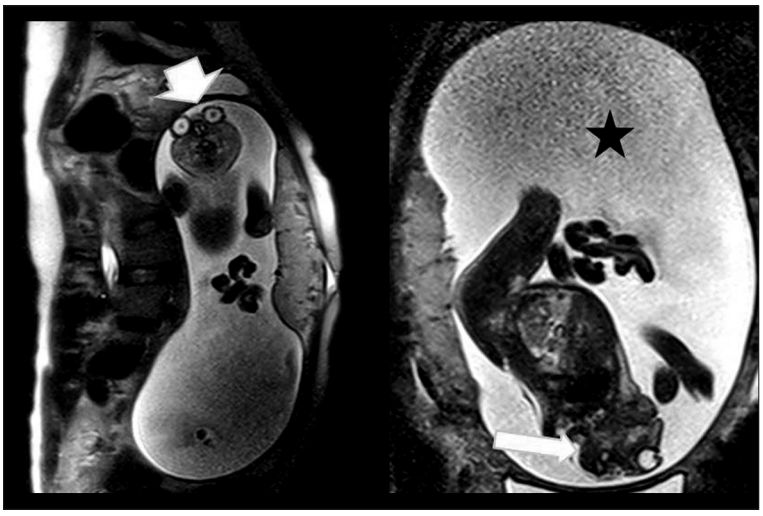

Figure 27. Fetal MR images demonstrating absent cranial bone/brain and bulging orbits (arrows). In addition, polyhydramnios is seen (star).

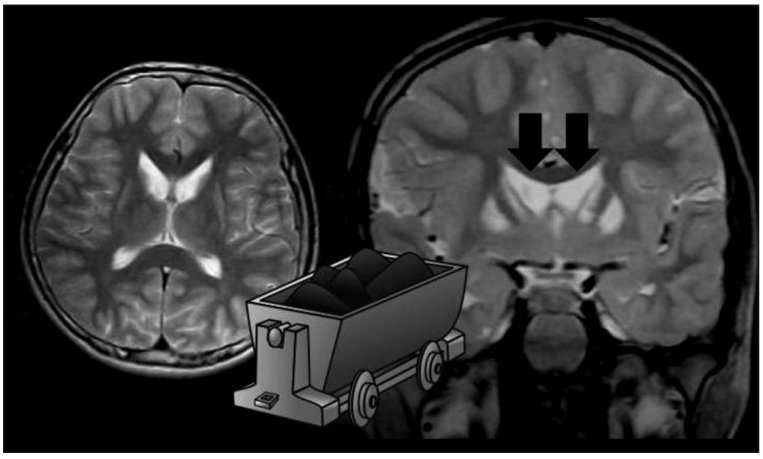

Figure 28. Axial T2-weighted MR image showing bilateral atrophy of caudate nuclei and compensatory dilatation of lateral ventricles, a finding known as "boxcar ventricle" (black arrow).

the temporal lobes and within the sylvian fissures (giving a "bat wing" appearance). Widening of the sylvian fissures is a very characteristic finding in glutaric aciduria type I (Figure 26) [30].

Frog eye appearance

Anencephaly is the most severe form of cranial neural tube defects (NTD) and is characterized by the absence of cortical tissue (although the brainstem and the cerebellum may be present) or cranial vault. Morphological spectrum within anencephaly ranges from holocrania (severest form) to merocrania (mildest form). Anencephaly may be radiologically detectable as early as at 11 weeks. A "frog eye" appearance may be seen in the coronal plane of US or MR images due to an absent cranial bone or brain, and bulging orbits (Figure 27) [31].

Boxcar ventricle sign

Huntington's disease is an autosomal dominant neurodegenerative disease, especially common in young adults. It has a course characterized by cognitive, behavioral, and muscle coordination disorders. In these cases, there may be an atrophy in basal ganglia, particularly in the caudate nucleus. Consequently, a widening may be seen in the frontal horns of the lateral ventricle. This particular appearance of frontal horns on multiplanar MR sections is called boxcar ventricle sign (Figure 28) [32].

Conclusions

Knowledge of classic neuroradiology signs and appearances of various central nervous system pathologies may be useful for differential diagnosis in daily practice.

References:

1. Chavhan GB, Shroof MM: Twenty classic signs in neuroradiology: a pictorial essay. Indian J Radiol Imaging, 2009; 19: 135–45
2. Tuncyurek O, Tarhan S, Orguc S et al: Computed tomographic reversal sign in an adult with methanol intoxication. J Clin Anal Med, 2012; 3: 359–60
3. Michel SJ: The Mount Fuji sign. Radiology, 2004; 232: 449–50
4. Thomas M: The lemon sign. Radiology, 2003; 228: 206–7
5. Rehman I, Bett Z, Husen Y et al: The 'molar tooth sign' in Joubert syndrome. J Pak Med Assoc, 2009; 59: 851–53
6. Mallick D, Thapa R: 'Molar tooth' sign in Joubert syndrome. Pediatr Radiol, 2010; 40: 131
7. Ghai S, Fong KW, Toi A et al: Prenatal US and MR imaging findings of lissencephaly: review of fetal cerebral sulcal development. Radiographics, 2006; 26: 389–405

8. Hitoshi S, Iwata M, Yoshikawa K: Mid-brain pathology of Wilson's disease: MRI analysis of three cases. J Neurol Neurosurg Psychiatry, 1991; 54: 624–26
9. Thapa R, Ghosh A: Face of the giant panda' sign in Wilson disease. Pediatr Radiol, 2008; 38: 1355
10. Bernauer TA: The radial bands sign. Radiology, 1999; 212: 761–62
11. Nandhagopal R, Krishnamoorthy SG: Neurological picture. Tigroid and leopard skin pattern of dysmyelination in metachromatic leukodystrophy. J Neurol Neurosurg Psychiatry, 2006; 77: 344
12. Kono T, Moriyama N, Tanaka R et al: Tigroid pattern of the white matter: a previously unrecognized MR finding in lissencephaly with cerebellar hypoplasia. Pediatr Radiol, 2008; 38: 1105–8
13. Masdeu JC, Quinto C, Olivera C et al: Open-ring sign: highly specific for atypical brain demyelination. Neurology, 2000; 54: 1427–33
14. Siddiqui A, Sahni A, Khadilkar S: The open-ring sign. Neurol India, 2005; 53: 253–54
15. Mullins ME: Modern emergent stroke imaging: pearls, protocols, and pitfalls. Radiol Clin North Am, 2006; 44: 41–62
16. Alaywan M, Chahine NA, Hage P, Nachanakian AK: Dandy-Walker malformation: Surgical treatment of 17 cases. PanArab J Neurosurg, 2008; 12: 25–30
17. Tan IL, van Schijndel RA, Pouwels PJ et al: MR venography of multiple sclerosis. Am J Neuroradiol, 2000; 21: 1039–42
18. Jang U, Lee K, Shim J et al: Diagnostic value of the cortical vein sign: unreliable index of atrophy on MR image. J Kor Neurotraumatol Soc, 2006; 2: 13–17
19. Saba PR: The caput medusae sign. Radiology, 1998; 207: 599–600
20. Boukobza M, Enjolras O, Guichard JP et al: Cerebral developmental venous anomalies associated with head and neck venous malformations. Am J Neuroradiol, 1996; 17: 987–94
21. Hadley DM: The Chiari malformations. J Neurol Neurosurg Psychiatr, 2002; 72: 38–40
22. Festa JR: Neurovascular Neuropsychology. Springer Verlag, 2009
23. Barkovich AJ, Jackson DE Jr, Boyer RS: Band heterotopias: A newly recognized neuronal migration anamoly. Radiology, 1989; 171: 455–58
24. Nicolaides KH, Campbell S, Gabbe SG et al: Ultrasound screening for spina bifida: cranial and cerebellar signs. Lancet, 1986; 12: 72–74
25. Shenoy C: Shapiro syndrome. QJM, 2008; 101: 61–62
26. Gebarski SS, Gebarski KS, Bowerman RA et al: Agenesis of the corpus callosum: sonographic features. Radiology, 1984; 151: 443–48
27. Akpinar E: The tram-track sign: cortical calcifications. Radiology, 2004; 231: 515–16
28. Oei AS, Vanzieleghem BD, Kunne MF: Diagnostic imaging and clinical finding in rhombencephalosynapsis: case report and literature review. JBR-BTR, 2001; 84: 197–200
29. Van beek EJ, Majoie CB: Case 25: Joubert syndrome. Radiology, 2000; 216: 379–82
30. Rai SP: Glutaric aciduria type1: CT diagnosis. J Pediatr Neurosci, 2009; 4: 143
31. Goldstein RB, Filly RA: Prenatal diagnosis of anencephaly: spectrum of sonographic appearances and distinction from the amniotic band syndrome. Am J Roentgenol, 1988; 151: 547–50
32. Mascalchi M, Lolli F, Della Nave R et al: Huntington disease: volumetric, diffusion-weighted, and magnetization transfer MR imaging of brain. Radiology, 2004; 30: 539–43